A Multi-cell Open-Loop Communication Approach to Ultra-Reliable Mobile Networks

Chun-Hung Liu*, Yu Luo*, and Lina Pu[†]
Department of Electrical and Computer Engineering, Mississippi State University, USA*
Department of Computer Science, University of Alabama, Tuscaloosa AL, USA[†]
e-mail: chliu@ece.msstate.edu; yu.luo@ece.msstate.edu; lina.pu@ua.edu

Abstract—Traditional means of achieving highly reliable wireless communications are to rely on a closed-loop communication methodology, which needs to implement complicated feedback communication mechanisms. Such closed-loop communication means inevitably incur feedback communication latency and thus lead to a fundamental tradeoff problem of simultaneously achieving high reliability and low latency. To avoid encountering this tradeoff problem, in this paper we adopt an open-loop communication methodology in a mobile network and propose a multi-cell association scheme to enhance the reliability of openloop communication. The multi-cell association scheme helps users connect to multiple base stations (BSs), which form a virtual cell of the user. We first characterize the distribution of the number of the users associating with a BS for the multicell association scheme and then use it to establish the accurate models of signal-to-interference ratios (SIRs) in the downlink and uplink. The downlink and uplink communication reliabilities, which are defined based on the SIRs in the downlink and uplink, are accurately analyzed and their explicit upper bounds are found. Our analytical and simulated results show that jointly adopting open-loop communication and multi-cell association is able to significantly improve the communication reliability of users, thereby creating an ultra-reliable mobile network.

I. INTRODUCTION

Traditional mobile wireless systems, such as long-term evolution (LTE) systems and its predecessors, were prominently designed to achieve the goal of high throughput in mobile communications, yet they can also achieve highly reliable communications in the physical layer at the expense of using complicated closed-loop protocol stack, which inevitably results in large networking latency. To reduce the end-toend latency in the wireless systems like LTE, it is necessary to fundamentally change their system architecture relying on the closed-loop communication and backbone links. This manifests the fact that there exists a tradeoff between high reliability and low latency in the system network architecture and subsequent communication protocols of mobile networks. Such a reliability-latency tradeoff problem intrinsically impedes the existing cellular systems to extend their services in mission-critical communication contexts with ultra highreliability and low-latency constraints, such as wireless control and automation in industrial environments, vehicle-tovehicle communications, and a tactile internet which allows controlling both real and virtual objects with real-time haptic feedback [1], [2].

To effectively reduce latency in 5G/6G systems, the essential approach is to adopt (feedback-free) open-loop communi-

cation so that no retransmission is needed and receivers can save time in performing additional processing and protocol. Open-loop communication has a distinct advantage to significantly reduce control signaling overhead for power control and channel estimation in cellular systems if compared with closed-loop communication. As such, in this paper we focus on how to fulfill ultra-reliable communications through openloop communication in a heterogeneous mobile network owing to the fact that extremely reliable open-loop communication is the key to low latency. All the existing works in the literature (for example, see [3]–[8]) are hardly dedicated to studying an open-loop methodology for ultra-reliable communication. Moreover, these prior works cannot reveal a good networkwide perspective on how interferences from other cells and user/cell association schemes impact the performance of ultrareliable communication in large wireless networks.

This paper aims to exploit the ultra-reliable performance of open-loop communication adopted in a large-scale mobile network. The contributions of this paper are summarized as follows. We propose to jointly adopt open-loop communication and multi-cell association in a heterogeneous mobile network so that the latency induced by closed-loop communication can be completely avoided and the communication reliability between BSs and users can be improved by spatial channel diversity rather than by feedback channel state information. We then derive the distribution of the number of the users associating with a BS in each tier of the network when the multi-cell association scheme is adopted. To the best of our knowledge, such a distribution is first found in this paper. Most importantly, it reveals that the void BS phenomenon still exists in the multi-cell scheme and needs to be considered in the analysis of ultra-reliable communication. The communication reliabilities of a user in the downlink and uplink are found for the non-collaborative and collaborative BS cases in a lowcomplexity form and they show that open-loop communication and multi-cell association indeed significantly improve the communication reliability of a user and make it achieve the target value of 99.999% when appropriately deploying BSs for a given user density.

II. SYSTEM MODEL AND PRELIMINARIES

Consider a heterogeneous mobile network comprised of two tiers of base stations (BSs) where the BSs in the same tier are of the same type and performance. We assume that the BSs in tier m are spatially distributed as an independent homogeneous Poisson point process (HPPP) \mathcal{B}_m of intensity λ_m , which can be expressed as

$$\mathcal{B}_m \triangleq \{B_{m,i} \in \mathbb{R}^2 : i \in \mathbb{N}\}, m = \{1, 2\},\tag{1}$$

where $B_{m,i}$ denotes the location of the BS i in tier m. Without loss of generality, the first tier is assumed to consist of the macrocell BSs and the second tier is assume to consist of small cell BSs. The transmit power of a macrocell BS is much larger than that of a small cell BS, whereas the density of the macrocell BSs is much smaller than that of the small cell BSs. In this mobile network, an anchor node which governs a number of nearby BSs according to the geographical deployment of the BSs is co-located with the edge/fog computing facilities, and a cloud radio access architecture comprised of a core network and a cloud is also employed in the mobile network. Each of the anchor nodes is connected to the core network, which can send complicated computing tasks to the cloud for advanced data processing. An illustrative model of the mobile network is depicted in Fig. 1. All users in the network also form an independent HPPP \mathcal{U} of density μ , which can be expressed as

$$\mathcal{U} \triangleq \{ U_j \in \mathbb{R}^2 : j \in \mathbb{N} \},\tag{2}$$

where U_j denotes the location of user j. In the mobile network, open-loop communication is adopted, that is, there is no feedback mechanism between BSs and users. Furthermore, we assume that all BSs and users are equipped with a single antenna. Such an assumption is made since no multi-antenna transmission gain can be optimally exploited on the transmitter side owing to open-loop communication. Without loss of generality, a typical user is assumed to be located at the origin and many following expressions and analyses are conducted according to the location of the typical user. In the following subsection, we will introduce the multi-cell association scheme that forms a virtual cell of a user and its related statistics.

A. Multi-cell Association and Its Related Statistics

Since open-loop communication is adopted in the mobile network, all the users in the network are allowed to associate with multiple BSs so that they can improve their communication reliability through spatial channel diversity. In addition, enabling users to associate with multiple BSs can significantly reduce the control signaling overhead due to frequent handovers between small cell BSs. This multicell association scheme helps a user form its virtual cell that contains all the BSs associated with the user. In other words, a virtual cell consists of a user and K BSs associated with the user. An illustration of a virtual cell with 3 BSs is shown in Fig. 1. In the following, we formulate the multi-cell association scheme and then study its statistical properties.

Suppose each user in the mobile network is able to associate with K BSs and we define V_k for all $k \in \mathbb{N}_+$ as

$$V_k \triangleq \arg \begin{cases} \max_{m,i:B_{m,i} \in \mathcal{B}} \left\{ \frac{w_m}{\|B_{m,i}\|^{\alpha}} \right\}, & k = 1\\ \max_{m,i:B_{m,i} \in \{\hat{\mathcal{B}}_{k-1}\}} \left\{ \frac{w_m}{\|B_{m,i}\|^{\alpha}} \right\}, & k > 1 \end{cases}, \quad (3)$$

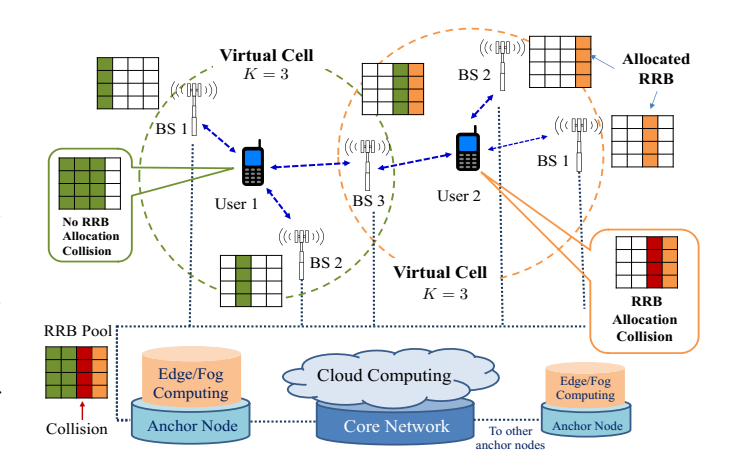


Fig. 1. The system model of a mobile network where two users associate with 3 base stations in their virtual cell. The two virtual cells share BS 3 and there is a collision when allocating radio resource blocks (RRBs) to User 2.

where $\mathcal{B} \triangleq \bigcup_{m=1}^2 \mathcal{B}_m$, $\hat{\mathcal{B}}_{k-1} = \mathcal{B} \backslash \bigcup_{j=1}^{k-1} V_j$, $\alpha > 2$ is the pathloss exponent, constant $w_m > 0$ is the tier-m cell association bias, and $\|X - Y\|$ denotes the Euclidean distance between nodes X and Y. According to (3), V_k can be viewed as the kth biased nearest BS to the typical user. For example, V_k is the kth nearest BS to the typical user if $\omega_m = 1$ for all $m \in \{1,2\}$. Let \mathcal{V}_K denote the set of the K BSs in the virtual cell of the typical user and it is called the virtual cell of the typical user denoted by $\mathcal{V}_K \triangleq \bigcup_{k=1}^K V_k$.

Since each user associates with K BSs, the number of users associating with the same BS is a random variable (RV), which dominates the resource allocation results of the BS and thereby impacts the communication reliability of users in their virtual cell. Finding the distribution of the number of users associating with a BS is crucial for the following analyses of communication reliability in a virtual cell. According to our previous works in [9] [10], the distribution of the number of users associating with a single BS is found (i.e., K=1). Applying the similar idea proposed in these two works, the distribution of the number of the users associating with a BS by using the multi-cell association scheme in (3) is found as shown in the following lemma.

Lemma 1. Suppose each user associates with K BSs by using the multi-cell association scheme in (3). Let N_m be the number of the users associating with a tier-m BS and the distribution of N_m can be accurately found as

$$p_{m,n} \approx \frac{\Gamma(n+\zeta_{m,K})}{n!\Gamma(\zeta_{m,K})} \cdot \frac{\left(\frac{K\mu}{\zeta_{m,K}\tilde{\lambda}_m}\right)^n}{\left(1 + \frac{K\mu}{\zeta_{m,K}\tilde{\lambda}_m}\right)^{(n+\zeta_{m,K})}}, \quad (4)$$

where $\Gamma(x) \triangleq \int_0^\infty t^{x-1} e^{-t} dt$ for x>0 is the Gamma function, $\zeta_{m,K}>0$ is a constant depending on K, $\widetilde{\lambda}_m \triangleq \sum_{i=1}^2 w_i^{\frac{2}{\alpha}} \lambda_i / w_m^{\frac{2}{\alpha}}$, and μ is the user density.

Proof: The proof is omitted since it is similar to the proof of Lemma 1 in [10].

To demonstrate how accurate $p_{m,n}$ in (4) is, the simulation results of $p_{m,n}$ are presented in Fig. 2 for a two-tier mobile

network. As can be seen in the figure, the numerical outcomes of $p_{m,n}$ in (4) perfectly coincide with their corresponding simulated results for $K=\{1,2,...,5\}$, and thereby $p_{m,n}$ in (4) is correct and very accurate. Lemma 1 reveals two important implications. First, it shows that the average number of users associating with a tier-m BS is $K\mu/\tilde{\lambda}_m$ and the tier-m average cell size is $K/\tilde{\lambda}_m$, which can be inferred from the results in [10] [11] so that the average cell size of the BSs adopting the multi-cell association scheme becomes K times larger than that of BSs adopting single-BS association. Second, the probability that a tier-m BS is not associated with any users, called tier-m void cell probability, can be readily found as

$$p_{m,0} = \left(1 + \frac{K\mu}{\zeta_{m,K}\widetilde{\lambda}_m}\right)^{-\zeta_{m,K}},\tag{5}$$

which indicates that the void probability would be considerably large in a dense mobile network with a moderate user density. As such, the void cell phenomenon needs to be considered in the interference model [9] [12] when the ratio of user density to small cell BS density is not fairly large.

B. The Truncated Shot Signal Process in a Virtual Cell

In this subsection, we would like to introduce the truncated shot signal process in a virtual cell, which pertains to the following reliability analyses. For the virtual cell of the typical user, the Kth-truncated shot signal process in it is defined as

$$S_K \triangleq \sum_{k=1}^K H_k W_k ||V_k||^{-\alpha}, \tag{6}$$

where H_k denote the channel gain of BS V_k , W_k is a nonnegative RV associated with V_k . Note that S_K only contains K shot signals from the K BSs in the virtual cell. Let $\mathcal{L}_Z(s) = \mathbb{E}[\exp(-sZ)]$ denote the Laplace transform of a non-negative RV Z for s>0 and $\mathcal{L}_{S_K}(s)$ can be derived as shown in the following lemma.

Theorem 1. If all the H_k 's of the Kth-truncated shot signal process in (6) are i.i.d. exponential RVs with unit mean (i.e., $H_k \sim \exp(1)$), then the Laplace transform of S_K can be explicitly found as

$$\mathcal{L}_{S_K}(s) = \exp\left[-\frac{\pi \widetilde{\lambda} s^{\frac{2}{\alpha}}}{\operatorname{sinc}(2/\alpha)}\right] \frac{(\pi \widetilde{\lambda})^K}{(K-1)!} \int_0^\infty y^{K-1} \times \exp\left\{\pi \widetilde{\lambda} y \left[1 + \ell \left(s y^{-\frac{\alpha}{2}}, \frac{2}{\alpha}\right)\right]\right\} dy, \quad (7)$$

where $\widetilde{\lambda} \triangleq \sum_{m=1}^2 w_m^{\frac{2}{\alpha}} \lambda_m$, $\vartheta_m \triangleq \mathbb{P}[W_k = w_m] = w_m^{\frac{2}{\alpha}} \lambda_m / \widetilde{\lambda}$ is the probability that a user associates with a tier-m AP, $\ell(y,z)$ for $y,z \in \mathbb{R}_+$ is defined as

$$\ell(y,z) \triangleq \frac{y^z}{\operatorname{sinc}(z)} - \int_0^1 \frac{y}{y + t^{\frac{1}{z}}} dt, \tag{8}$$

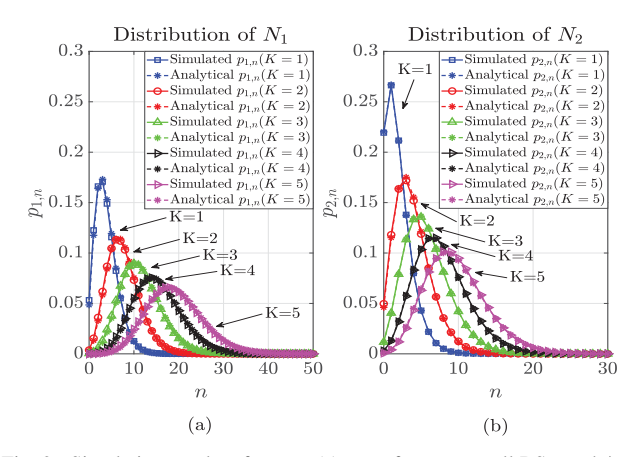


Fig. 2. Simulation results of $p_{m,n}$: (a) $p_{1,n}$ for macro cell BSs, and $\zeta_{1,K}=\{3.60,6.04,7.91,9.43,10.65\}$, for $K=\{1,2,...,5\}$ (b) $p_{2,n}$ for small cell BSs, and $\zeta_{2,K}=\{3.5,5.49,7.19,8.58,9.68\}$, for $K=\{1,2,...,5\}$. The network parameters for both simulations are: $\lambda_1=1\times 10^{-6}$ (macro BSs/m²), $\lambda_2=5\times 10^{-5}$ (small cell BSs/m²), $\mu=1\times 10^{-4}$ (users/m²), $P_1=20$ W, $P_2=5$ W.

and $\mathrm{sinc}(x) \triangleq \frac{\sin(\pi x)}{\pi x}$. In addition, the upper bound on $\mathbb{P}[S_K \geq y]$ can be found as

$$\mathbb{P}[S_K \ge y] \le 1 - \prod_{k=1}^K \left[1 - \mathcal{L}_{Y_k^{\frac{\alpha}{2}}} \left(\frac{2ky}{K(K+1)} \right) \right], \quad (9)$$

where $Y_k \sim \text{Gamma}(k, \pi \widetilde{\lambda})$ is a Gamma RV with shape parameter k and rate parameter $\pi \widetilde{\lambda}$.

The results in Theorem 1 will play a key role in analyzing the communication reliability in a virtual cell.

III. COMMUNICATION RELIABILITY ANALYSIS

In this section, the uplink and downlink communication reliabilities in a virtual cell will be investigated. The orthogonal frequency division multiple access is assumed to be employed in the network and the analyses of uplink and downlink communication reliabilities are proceeded in accordance with how the RRBs in the cell of each BS are allocated to users. We will first specify how users access the RRBs of a BS and then analyze the uplink communication reliability. Afterwards, we will continue to study the communication reliability in the downlink.

A. Analysis of Uplink Communication Reliability

According to the multi-cell association scheme and the virtual cell of a user specified in the previous section, our interest here is to study how likely a user is able to successfully access available RBs of a BS and then send its message to the K BSs in its virtual cell through uplink open-loop communication. To establish the uplink access from a user to the K BSs, we propose the following radio resource allocation scheme for uplink open-loop communication:

• To let a user have good uplink connections, the user forms its virtual cell by associating with its first K nearest BSs. Hence, all the cell association biases in (3) are unity, i.e., $w_m=1$ for all $m\in\{1,2\}$.

- Each RRB serves as the basic unit while scheduling radio resources. Multiple RRBs in a single time slot are mapped to a single radio resource unit for transmitting a message. Users are allowed to transmit one message in each time slot.
- Due to open-loop communication, there is no channel state information of each BS available in a virtual cell. A user accesses the radio resource in a distributed manner, that is, it has to randomly select RRUs for the K BSs in its virtual cell.

The uplink transmission collisions, which fails the uplink communication, may occur in the cell of a BS because users in the cell of the BS may select the same uplink RRUs. The probability that there is no uplink collision in a virtual cell is referred as the uplink non-collision reliability, which is found in the following lemma.

Lemma 2. If the probability that the user selects any one of the RRBs for each BS in its virtual cell is $\delta \in (0,1)$, then the uplink non-collision reliability of each BS in its virtual cell is found as

$$\rho^{ul} = \sum_{m=1}^{2} \vartheta_m \sum_{n=1}^{\infty} p_{m,n} (1 - \delta)^{n-1}, \tag{10}$$

where $\vartheta_m = \lambda_m / \sum_{i=1}^2 \lambda_i$ is the probability that an BS in the virtual cell is from \mathcal{B}_m . Hence, the uplink non-collision reliability of the user in its virtual cell is

$$\rho_K^{ul} = 1 - \left[1 - \rho^{ul}\right]^K. \tag{11}$$

Proof: See Appendix B.

From lemma 2, we can learn that the uplink non-collision reliability of each BS ρ^{ul} is mainly affected by δ and K. It is worth noting that increasing K does not always improve ρ^{ul}_K since more users may associate with the same BS and ρ^{ul} reduces accordingly.

If the mobile network is interference-limited, the uplink signal-to-interference ratio (SIR) of the kth BS in the virtual cell of the typical user can be defined as

$$\gamma_k^{ul} \triangleq \frac{h_k q_k ||V_k||^{-\alpha}}{\sum_{j:U_j \in \mathcal{U}_a} h_j q_j ||V_k - U_j||^{-\alpha}},$$
 (12)

where $h_k \sim \exp(1)$ denotes the uplink fading channel gain from the typical user to BS V_k , q_k is the transmit power used by the typical user for BS V_k , q_j is the transmit power of user U_j , and h_j is the uplink fading channel gain from U_j to V_k . $\mathcal{U}_a \subseteq \mathcal{U}$ represents the set of the actively transmitting users using the same RRU as the typical user. According to (12), we consider the following two cases: non-collaborative and collaborative BSs in the virtual cell. The case of non-collaborative BSs is referred to as the scenario that the BSs in the virtual cell are not perfectly coordinated so that they cannot jointly perform coordinated multi-point (CoMP) reception/transmission. In contrast, the collaborative BSs are able to jointly perform CoMP. Hence, the uplink communication reliability of a virtual cell in the non-collaborative case is

defined as the probability that a message is successfully received by at least one BS in the virtual cell, which can be written as

$$\eta_K^{ul} \triangleq \mathbb{P}\left[\max_{k \in \{1, \dots, K\}} \{\gamma_k^{ul} \mathbb{1}(V_k \in \mathcal{V}_K^{nc})\} \ge \theta\right], \quad (13)$$

where $\mathbb{1}(\mathcal{A})$ denotes the indicator function that is unity if event \mathcal{A} is true and zero otherwise. $\theta > 0$ is the SIR threshold for successful decoding and $\mathcal{V}_K^{nc} \subseteq \mathcal{V}_K$ is the subset of the BSs without collision in set \mathcal{V}_K . For the case of collaborative BSs, the uplink communication reliability of a virtual cell is defined as

$$\eta_K^{ul} \triangleq \mathbb{P}\left[\frac{S_K^{ul}}{\sum_{j:U_j \in \mathcal{U}_a \setminus \mathcal{V}_K} h_j q_j \|V_k - U_j\|^{-\alpha}} \ge \theta\right], \quad (14)$$

where $S_K^{ul} \triangleq \sum_{k:V_k \in \mathcal{V}_K^{nc}} h_k q_k \|V_k\|^{-\alpha}$. Namely, η_K^{ul} in (14) is the probability that the non-collision BSs in the virtual cell jointly and successfully decode the uplink message. For the sake of analytical tractability, we consider that non-coherent signal combing happens among all the non-collision BSs in the virtual cell. The analytical results of (13) and (14) are summarized in the following theorem.

Theorem 2. If all the K BSs in the virtual are unable to collaborate, the uplink communication reliability defined in (13) is accurately found as

$$\eta_K^{ul} \approx 1 - \prod_{k=1}^K \left\{ 1 - \rho^{ul} \left(1 + \frac{\delta \theta^{\frac{2}{\alpha}} (1 - p_0)}{\operatorname{sinc}(2/\alpha)} \right)^{-k} \right\},$$
(15)

where $p_0 \triangleq p_{m,0}$ that is given in (5) with $w_m = 1$ for $m \in \{1,2\}$. When all the K BSs in the virtual cell are able to collaborate to jointly decode the uplink message, η_K^{ul} in (14) can be upper bounded by

$$\eta_K^{ul} \le \rho^{ul} \left\{ 1 - \prod_{k=1}^K \left[1 - \frac{1}{\left(1 + \frac{\delta(1 - p_0)}{\operatorname{sinc}(2/\alpha)} \left(\frac{2k\theta}{K(K+1)}\right)^{\frac{2}{\alpha}}\right)^k} \right] \right\}.$$
(16)

Proof: See Appendix C.

Theorem 2 reveals that η_K^{ul} in (15) monotonically increases as K increases. However, increasing K suffers from the diminishing returns problem of the uplink communication reliability; i.e., associating with too many BSs is not efficient to improve η_K^{ul} for a user. In addition to increasing K, reducing the probability of scheduling each RRU and densely deploying BSs in the mobile network are alternative efficient approaches to further enhancing η_K^{ul} .

B. Analysis of Downlink Communication Reliability

In this subsection, we focus on the analysis of the downlink communication reliability of a user in its virtual cell. In the downlink, each user is assumed to associate with the first K strongest BSs (i.e., $\omega_m = P_m$ in (3)) and each downlink RRB of a BS is only assigned to one user associating with the BS.

Now consider the case of non-collaborative BSs in a virtual cell and define the downlink SIR of the typical user as

$$\gamma_k^{dl} \triangleq \frac{H_k Q_k ||V_k||^{-\alpha}}{I_{\mathcal{V}_K,k}^{\mathsf{Intra}} + I_{\mathcal{V}_K}^{\mathsf{Inter}}},\tag{17}$$

where $I_{\mathcal{V}_K,k}^{\text{Intra}} = \sum_{i:V_i \in \mathcal{V}_K \setminus V_k} H_i Q_i \|V_i\|^{-\alpha}$ denotes the intravirtual-cell interference received by the typical user in its virtual cell, $I_{\mathcal{V}_K}^{\text{Inter}} = \sum_{m,i:B_{m,i} \in \mathcal{B} \setminus \mathcal{V}_K} O_{m,i} h_{m,i} P_m \|B_{m,i}\|^{-\alpha}$ is the inter-cell interference from the BSs that are not in the virtual cell, $Q_k \in \{P_1, P_2\}$ is the transmit power of the BS V_k , H_k and $h_{m,i}$ are the downlink channel fading gains which are from V_k and $B_{m,i}$ to the typical user, respectively. $O_{m,i}$ is a Bernoulli RV that is unity if $B_{m,i}$ is not void and zero otherwise. Note that $\mathbb{P}[O_{m,i}=1]=1-p_{m,0}$ and it can be found by (5). In such a case, the downlink communication reliability of a virtual cell with K BSs is defined as

$$\eta_K^{dl} \triangleq \mathbb{P}\left[\max_{k \in \{1, \dots, K\}} \{\gamma_k^{dl}\} \ge \theta\right],$$
(18)

which is the probability that at least one BS in the virtual cell successfully transmits message to the user. On the other hand, if all the K BSs in the virtual cell collaborate to eliminate the intra-virtual-cell interference, the downlink communication reliability can be simply written as

$$\eta_K^{dl} = \mathbb{P}\left[\frac{\sum_{k=1}^K H_k Q_k ||V_k||^{-\alpha}}{I_{\mathcal{V}_K}^{\text{Inter}}} \ge \theta\right]. \tag{19}$$

The explicit upper bounds on η_K^{dl} defined in (18) and (19) are found in the following theorem.

Theorem 3. If all the BSs in a virtual cell are not coordinated, the downlink communication reliability in (18) is explicitly upper bounded by

$$\eta_K^{dl} \le 1 - \prod_{k=1}^K \left\{ 1 - \left[1 + \delta \ell \left(\theta, \frac{2}{\alpha} \right) \bar{\vartheta} \right]^{-k} \right\},$$
(20)

where $\bar{\vartheta} \triangleq \sum_{m=1}^2 \vartheta_m (1-p_{0,m}), \ \vartheta_m \triangleq P_m^{2/\alpha} \lambda_m / \widetilde{\lambda}, \ and \ \widetilde{\lambda} = \sum_{m=1}^2 P_m^{\frac{2}{\alpha}} \lambda_m$. For the case of collaborative BSs, the upper bound on η_K^{dl} in (19) can be found as

$$\eta_K^{dl} \le 1 - \left\{ 1 - \left[1 + \delta \ell \left(\frac{\theta}{K^{\frac{\alpha}{2} + 1}}, \frac{2}{\alpha} \right) \bar{\vartheta} \right]^K \right\}^{-K}. \tag{21}$$

Proof: The proof is omitted since it is similar to the proof of Theorem 2.

According to the results in Theorem 3, increasing K indeed improves η_K^{dl} , yet it also leads to the diminishing returns problem, like the uplink communication reliability. When K is not large, densely deploying BSs may remarkably boost η_K^{dl} in that it makes $p_{m,0}$ increase. Furthermore, η_K^{dl} in (21) reveals some insights into how to schedule resources and deploy BSs in the mobile network so as to achieve the predesignated target value of η_K^{dl} .

TABLE I NETWORK PARAMETERS FOR SIMULATION [7], [13]

| Parameter\BS Type (Tier m) | Macrocell BS (1) | Small cell BS (2) |
|--|---|---|
| Transmit Power P_m (W) | 20 | 5 |
| User Density μ (users/m ²) | 5×10^{-5} | |
| BS Density λ_m (BSs/m ²) | 1×10^{-6} | $[0.1\mu, \mu]$ |
| RRU Selection Probability δ | 0.05 | |
| Path-loss Exponent α | 4 | |
| Tier- m Association Bias w_m | $1(Uplink), P_m(Downlink)$ | |
| Bandwidth B | 20 MHz | |
| Packet Size ξ (bytes) | 8, 32, and 64 | |
| Transmission Duration τ (ms) | 0.05 | |
| Decoding Error Probability ϵ | 2×10^{-8} | |
| SIR Threshold θ | $\exp\left[\frac{\xi \ln 2}{\tau B} +\right]$ | $\left[\frac{Q_G^{-1}(\epsilon)}{\sqrt{\tau B}}\right] - 1$ |

IV. NUMERICAL RESULTS

In this section, some numerical results are provided to numerically validate the analytical results of the uplink communication reliability of a virtual cell with short packet transmission. The network parameters for simulation is shown in Table I. To clearly show whether or not the target communication reliability of 99.999% is attained in the uplink and downlink, the simulation results of the uplink and downlink outage probabilities (i.e., $1 - \eta_K^{ul}$ and $1 - \eta_K^{dl}$) are shown in the following figures and the designated outage threshold is thus $1 - 99.999\% = 10^{-5}$. Since the simulation of the uplink and downlink outages is rare-event, it is terminated as the outage event occurs over 200 times so that we can obtain much confident statistics. Due to considering short packet transmission, we adopt the maximum achievable rate of short blocklength regime without considering channel dispersion found in [7], [13] to infer the outage condition for the mobile network as follows:

$$\ln(1 + \operatorname{SIR}_K^{ul}) - \frac{Q_G^{-1}(\epsilon)}{\sqrt{\pi R}} \le \frac{\xi}{R\tau},\tag{22}$$

where SIR_K^{ul} is equal to $\max_{k\in\{1,\dots,K\}}\{\gamma_k^{ul}\mathbb{1}(V_k\in\mathcal{V}_K^{nc})\}$ for uplink and $\max_{k\in\{1,\dots,K\}}\{\gamma_k^{dl}\}$ for downlink, $Q_G^{-1}(\cdot)$ stands for the inverse of (Gaussian) Q-function, ξ denotes the size of a short packet, and τ is the duration of transmission. The inequality in (22) can be further rewritten as

$$\operatorname{SIR}_{K}^{ul} \le \exp\left(\frac{Q_{G}^{-1}(\epsilon)}{\sqrt{\tau B}} + \frac{\xi}{B\tau}\right) - 1.$$
 (23)

Thus, we can get the uplink reliability of short packet transmission, i.e., $\eta_K^{ul} = \mathbb{P}[\mathrm{SIR}_K^{ul} \geq \theta]$ by setting the SIR threshold as $\theta = \exp\left(\frac{Q_G^{-1}(\epsilon)}{\sqrt{\tau B}} + \frac{\xi}{B\tau}\right) - 1$, as shown in Table I.

The numerical results of the uplink outage probabilities are shown in Figure 3. The analytical results corresponding to this scenario in the figure are found by using (15). As shown in Fig. 3(a), $1 - \eta_K^{ul}$ increases (η_K^{ul} decreases) as μ/λ_2 increases. This is because more co-channel interference is created as μ/λ_2 gets larger so that more BSs are associated with users and become active. The short packet transmission with a longer packet size makes the outage probability increase, which can be mitigated by decreasing μ/λ_2 . Also, all the simulated results are very close to their corresponding

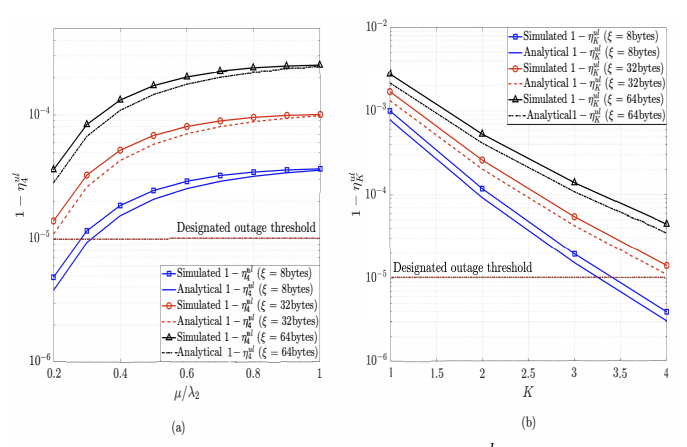


Fig. 3. Numerical results of the uplink outage $1-\eta_K^{ul}$ for the case of non-collaborative BSs: (a) $1-\eta_K^{ul}$ versus μ/λ_2 for K=4, (b) $1-\eta_K^{ul}$ versus K for $\mu/\lambda_2=0.5$ (users/small cell BS) and $\lambda_2=250$ (BSs/km²).

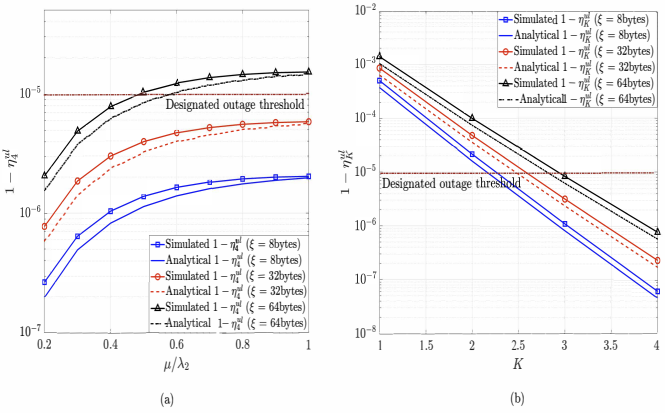


Fig. 4. Numerical results of the uplink outage $1-\eta_K^{ul}$ for the scenario of collaborative BSs: (a) $1-\eta_K^{ul}$ versus μ/λ_2 for K=4, (b) $1-\eta_K^{ul}$ versus K for $\mu/\lambda_2=0.5$ (users/small cell BS) and $\lambda_2=250$ (BSs/km²).

analytical results, which validates that the analytical result in (15) is still fairly accurate even when the received uplink SIRs at different BSs are assumed to be independent when deriving (15). Figure 3(b) illustrates how the uplink outage probability is suppressed as the number of BSs in virtual cell increases. As shown in the figure, $1 - \eta_K^{ul}$ significantly reduces as K increases from 1 to 4, but only the case of the blue curves is able to achieve the outage probability below the designated outage threshold when K > 4. In light of this, users are suggested to associate with more BSs and/or reduce their packet size. The simulated results of the uplink outage probabilities for the scenario of collaborative BSs are shown in Fig. 4 in which the analytical results that are the lower bound on the outage probability are calculated by using (16). Only the results of the black curves in Fig. 4(a) are above the designated outage threshold of 10^{-5} and thereby all the results in Fig. 4(a) are much better than those in Fig. 3(a). This reveals that we do not need to deploy many BSs to significantly decrease $1 - \eta_K^{ul}$ when the BSs are able to collaborate. In Fig. 4(b), the simulated outcomes are also much better than those in Fig. 3(b), which indicates that multi-cell association should be jointly implemented with CoMP so as to better serve the ultra-reliable traffic.

V. CONCLUSION

This paper provides a viable solution of using open-loop communication and multi-cell association to the longstanding tradeoff problem between communication reliability and latency due to closed-loop communication. The multi-cell association scheme and open-loop communication in a mobile network are proposed and how much the communication reliability of a virtual cell achieved by them is analyzed. Our analytical outcomes and numerical results show that the proposed open-loop communication and multi-cell association scheme are able to achieve the target communication reliability provided that the BSs are sufficiently deployed and the number of the BSs in a virtual cell is properly chosen.

APPENDIX

A. Proof of Theorem 1

Let $S_{\infty} = \lim_{K \to \infty} S_K$ and $S_{-K} = S_K - S_{\infty}$. Thus, S_{-K} can be alternatively written as

$$S_{-K} = \sum_{i=K+1}^{\infty} \frac{H_i W_i}{\|V_i\|^{\alpha}} \stackrel{d}{=} \sum_{j: \widetilde{V}_i \in \widetilde{\mathcal{B}}} H_j (\|\widetilde{V}_K\|^2 + \|\widetilde{V}_j\|^2)^{-\frac{\alpha}{2}},$$

where $\stackrel{d}{=}$ denotes the equivalence in distribution, $\widetilde{\mathcal{B}} \triangleq \{\widetilde{V}_j \in \mathbb{R}^2 : \widetilde{V}_j = W_j V_j, V_j \in \mathcal{B}, j \in \mathbb{N}_+ \}$ is a homogeneous PPP of density $\widetilde{\lambda}$, and $\|\widetilde{V}_{j+i}\|^2 = \|\widetilde{V}_j\|^2 + \|\widetilde{V}_i\|^2$ for all $i,j \in \mathbb{N}_+$ and $i \neq j$ based on the proof of Proposition 1 in [14]. Therefore, the Laplace transform of S_{-K} can be calculated as shown in the following:

$$\begin{split} \mathcal{L}_{S_{-K}}(s) &= \mathbb{E}\left[\exp\left(\frac{-s}{\|\widetilde{V}_K\|^{\alpha}} \sum_{j:\widetilde{V}_j \in \widetilde{\mathcal{B}}} \frac{H_j}{\left(1 + \frac{\|\widetilde{V}_j\|^2}{\|\widetilde{V}_K\|^2}\right)^{\frac{\alpha}{2}}}\right)\right] \\ &\stackrel{(a)}{=} \mathbb{E}_{Y_K}\left[\exp\left(-\pi\widetilde{\lambda} \int_0^{\infty} \mathbb{E}_H\left[1 - e^{HsY_K^{-\frac{\alpha}{2}}(1 + \frac{r}{Y_K})^{-\frac{\alpha}{2}}}\right] \mathrm{d}r\right)\right] \\ &\stackrel{(b)}{=} \mathbb{E}_{Y_K}\left[\exp\left(-\pi\widetilde{\lambda} Y_K \int_1^{\infty} \mathbb{P}\left[Y_K r' \leq \left(\frac{sH}{Z}\right)^{\frac{2}{\alpha}}\right] \mathrm{d}r'\right)\right] \\ &\stackrel{(c)}{=} \mathbb{E}_{Y_K}\left\{\exp\left[-\pi\widetilde{\lambda} Y_K \ell \left(\frac{s}{Y_K^{\frac{\alpha}{2}}}, \frac{2}{\alpha}\right)\right]\right\}, \end{split}$$

where $\stackrel{(a)}{=}$ follows from the probability generating functional (PGFL) of the homogeneous PPP $\widetilde{\mathcal{B}}$ [15] and $Y_k \triangleq \|\widetilde{V}_k\|^2$, (b) is obtained by using $Z \sim \exp(1)$, and (c) is obtained by using the derivation technique in the proof of Proposition 2 in [12]. Since $\mathcal{L}_{S_{\infty}}(s) = \mathbb{E}\left[e^{-sS_K}\right] \mathbb{E}\left[e^{-sS_{-K}}\right] = \exp\left[-\frac{\pi \widetilde{\lambda} s^{\frac{2}{\alpha}}}{\sin(2/\alpha)}\right]$, $\mathcal{L}_{S_K}(s)$ can be found as shown in (7). Also, the proof of the result in (9) is omitted due to limited space.

B. Proof of Lemma 2

Let M_k denote the number of the users associating with the kth BS in the virtual cell. The probability of no collisions happening in the cell of the kth BS is $\delta(1-\delta)^{M_k-1}$ if the probability of a user selecting any one of the RRUs for each BS is δ . Suppose the radio resource (available

bandwidth) of each BS can be divided into R radio resource units so that we have $\delta=\frac{1}{R}.$ Thus, the probability that a BS in the virtual cell does not have collisions, denoted by $\rho^{ul}=\sum_{r=1}^R \delta\,\mathbb{E}\left[(1-\delta)^{M_k-1}\right]$, can be written as

$$\rho^{ul} = \sum_{r=1}^{R} \frac{1}{R} \mathbb{E} \left[(1 - \delta)^{M_k - 1} \right] = \mathbb{E} \left[(1 - \delta)^{M_k - 1} \right],$$

where $\mathbb{E}[(1-\delta)^{M_k-1}] = \sum_{m=1}^2 \mathbb{P}[V_k \in \mathcal{B}_m] \mathbb{E}[(1-\delta)^{M_k-1}|V_k \in \mathcal{B}_m]$ and we thus have $\rho^{ul} = \sum_{m=1}^2 \vartheta_m \mathbb{E}\left[(1-\delta)^{N_m-1}\right] = \sum_{m=1}^2 \vartheta_m \sum_{n=1}^\infty p_{m,n}(1-\delta)^{n-1}$ where $\vartheta_m = \mathbb{P}[V_k \in \mathcal{B}_m]$ and N_m is the number of the users associating with a tier-m BS. Moreover, we know that the probability that the nearest BS to the user located at the origin is from the mth tier is $\mathbb{P}[\|B_{m,*}\|^{-\alpha} \geq \|B_{i,*}\|^{-\alpha}] = \mathbb{P}[\|B_{m,*}\|^2 \leq \|B_{i,*}\|^2]$ for $m \neq i$ in which $B_{i,*}$ is the nearest point in \mathcal{B}_i to the user. Since $c^{-1}\|B_{m,*}\|^2 \sim \exp(c\pi\lambda_m)$ for any c>0, we thus have $\vartheta_m = \mathbb{P}\left[\|B_{m,*}\|^2 \leq \|B_{k,*}\|^2\right] = \frac{\lambda_m}{\sum_{i=1}^m \lambda_i}$. Substituting the above result of ϑ_m into the above expression of ρ^{ul} yields the result in (10). In addition, the uplink non-collision reliability of the user is the probability that there is at least one non-collision BS in the virtual and thereby it can be expressed as $\rho_K^{ul} = 1 - (1 - \rho^{ul})^K$, which is equal to the result in (11) by substituting the result of ρ^{ul} in (10) into ρ_K^{ul}

C. Proof of Theorem 2

First consider the scenario in which all K BSs in the virtual cell do not collaborate and the transmit power q of users is equally allocated to the K BSs, i.e., $q_i = q_k = q/K$ for all $i \in \mathbb{N}_+$ and $k \in \{1, \ldots, K\}$. If all the non-collision uplink SIRs in (13) are independent, we have

$$\eta_K^{ul} = 1 - \mathbb{P}\left[\max_{k \in \{1, \dots, K\}} \{\gamma_k^{ul} \mathbb{1}(V_k \in \mathcal{V}_K^{nc})\} \le \theta\right]$$

$$\stackrel{(a)}{=} 1 - \prod_{k=1}^K \{1 - \rho^{ul} \mathbb{P}\left[\gamma_k^{ul} \ge \theta\right]\},$$

where (a) follows from the result of $\mathbb{P}[\mathbb{1}(V_k \in \mathcal{V}_K^{nc}) = 1] = \sum_{m=1}^2 \vartheta_m \sum_{n=1}^\infty p_{m,n} (1-\delta)^{n-1} = \rho^{ul}$. Whereas $\mathbb{P}[\gamma_k^{ul} \geq \theta]$ can be derived as shown in the following:

$$\mathbb{P}[\gamma_k^{ul} \ge \theta] \stackrel{(b)}{=} \mathbb{E}\left[\exp\left(-\theta \|V_k\|^{\alpha} \sum_{j:U_j \in \mathcal{U}_a} \frac{h_j}{\|U_j\|^{\alpha}}\right)\right]$$

$$\stackrel{(c)}{=} \mathbb{E}_{\|V_k\|^2} \left[e^{-\frac{\pi \theta^{\frac{2}{\alpha}} \|V_k\|^2 \mu_a}{\operatorname{sinc}(2/\alpha)}}\right] \stackrel{(d)}{=} \left(1 + \frac{\theta^{\frac{2}{\alpha}} \mu_a}{\operatorname{sinc}(2/\alpha)\widetilde{\lambda}}\right)^{-k},$$

where (b) follows from $h_k \sim \exp(1)$ and the Slivnyak theorem saying that the statistical property of a homogeneous PPP evaluated at V_k is the same as that evaluated at the origin (or any point in the network) [11], [15], (c) is obtained by first applying the PGFL of an HPPP to \mathcal{U}_a that is an HPPP of density $\mu_a = \delta(1-p_0)\sum_{m=1}^2 \lambda_m = \delta(1-p_0)\widetilde{\lambda}$, and (d) is due to $\|V_k\|^2 \sim \operatorname{Gamma}(k,\pi\widetilde{\lambda})$. Then substituting the result of $\mathbb{P}[\gamma_k^{ul} \geq \theta]$ into the result of η_K^{ul} found in (a) leads to the

result in (15). Next, the upper bound on η_K^{ul} in (14) can be thereupon derived as follows:

$$\eta_K^{ul} \stackrel{(e)}{=} \rho^{ul} \mathbb{P} \left[\sum_{k:V_k \in \mathcal{V}_K} \frac{h_k}{\|V_k\|^{\alpha}} \ge \theta \sum_{j:U_j \in \mathcal{U}_a} \frac{h_j}{\|U_j\|^{\alpha}} \right] \stackrel{(f)}{\le} \rho^{ul} \left\{ 1 - \prod_{k=1}^K \left(1 - \mathbb{E}_{Y_k} \left[\exp\left(\frac{-\pi \mu_a Y_k}{\operatorname{sinc}(2/\alpha)} \left(\frac{2k\theta}{K(K+1)}\right)^{\frac{2}{\alpha}} \right) \right] \right) \right\},$$

where (e) follows from $\mathbb{P}[\mathbb{1}(V_k \in \mathcal{V}_K^{nc})] = \rho^{ul}$ and $q_j = q/K$ for all j and (f) follows from the result in (9) for $w_m = 1$. Thence, using $\mathbb{E}_{Y_k}[\exp(-sY_k)] = (1 + s/\pi \widetilde{\lambda})^{-k}$ for s > 0 and substituting $\mu_a = \delta(1 - p_0)\widetilde{\lambda}$ into the above result of η_K^{ul} yield the result in (16).

REFERENCES

- [1] M. Simsek et al., "5G-enabled tactile internet," IEEE J. Select. Areas Commun., vol. 34, no. 3, pp. 460–473, Mar. 2016.
- [2] S.-Y. Lien, S.-C. Hung, K.-C. Chen, and Y.-C. Liang, "Ultra-low latency ubiquitous connections in heterogeneous cloud radio access networks," *IEEE Wireless Commun. Mag.*, vol. 22, no. 3, pp. 22–31, Mar. 2015.
- [3] A. Avranas, M. Kountouris, and P. Ciblat, "Energy-latency tradeoff in ultra-reliable low-latency communication with retransmissions," *IEEE J. Select. Areas Commun.*, vol. 36, no. 11, pp. 2475–2485, Nov. 2018.
- [4] B. Lee, S. Park, D. J. Love, H. Ji, and B. Shim, "Packet structure and receiver design for low latency wireless communications with ultra-short packets," *IEEE Trans. Wireless Commun.*, vol. 16, no. 2, pp. 796–807, Feb. 2018.
- [5] J. P. B. Nadas, O. Onireti, R. D. Souza, and H. Alves, "Performance analysis of hybrid ARQ for ultra-reliable low latency communications," *IEEE Sensors J.*, vol. 19, no. 9, pp. 3521–3531, Nov. 2019.
- [6] R. Devassy, G. Durisi, G. C. Ferrante, O. Simeone, and E. Uysal, "Reliable transmission of short packets through queues and noisy channels under latency and peak-age violation guarantees," *IEEE J. Select. Areas Commun.*, vol. 37, no. 4, pp. 721–734, Apr. 2019.
- [7] C. Sun, C. She, C. Yang, T. Q. S. Quek, Y. Li, and B. Vucetic, "Optimizing resource allocation in the short blocklength regime for ultra-reliable and low-latency communications," *IEEE Trans. Wireless Commun.*, vol. 18, no. 1, pp. 402–415, Jan. 2019.
- [8] T. H. Jacobsen, R. Abreu et al., "Multi-cell reception for uplink grant-free ultra-reliable low-latency communications," *IEEE Access*, vol. 7, pp. 80 208–80 218, Jun. 2019.
- [9] C.-H. Liu and L.-C. Wang, "Random cell association and void probability in poisson-distributed cellular networks," in *IEEE Int. Conf. Commun.*, Jun. 2015, pp. 2816–2821.
- [10] C.-H. Liu and K. L. Fong, "Fundamentals of the downlink green coverage and energy efficiency in heterogeneous networks," *IEEE J. Select. Areas Commun.*, vol. 41, no. 12, pp. 3271–3287, Dec. 2016.
- [11] S. N. Chiu, D. Stoyan, W. S. Kendall, and J. Mecke, Stochastic Geometry and Its Applications, 3rd ed. New York: John Wiley and Sons, Inc., 2013
- [12] C.-H. Liu and L.-C. Wang, "Optimal cell load and throughput in green small cell networks with generalized cell association," *IEEE J. Select. Areas Commun.*, vol. 34, no. 5, pp. 1058–1072, May 2016.
- [13] W. Yang, G. Durisi, T. Koch, and Y. Polyanskiy, "Quasi-static multipleantenna fading channels at finite blocklength," *IEEE Trans. Inform. Theory*, vol. 60, no. 7, pp. 4232–4265, 2014.
- [14] C.-H. Liu and D.-C. Liang, "Heterogeneous networks with power-domain NOMA: Coverage, throughput and power allocation analysis," *IEEE Trans. Wireless Commun.*, vol. 17, no. 5, pp. 3524–3539, May 2018.
- [15] F. Baccelli and B. Błaszczyszyn, "Stochastic geometry and wireless networks: Volume I: Theory," Foundations and Trends in Networking, vol. 3, no. 3-4, pp. 249–449, 2010.